

LEGIBILITY NOTICE

A major purpose of the Technical Information Center is to provide the broadest dissemination possible of information contained in DOE's Research and Development Reports to business, industry, the academic community, and federal, state and local governments.

Although a small portion of this report is not reproducible, it is being made available to expedite the availability of information on the research discussed herein.

LA-UR--88-3845

DE89 003495

TITLE ONCE-THROUGH STEAM-GENERATOR SENSITIVITY CALCULATIONS

AUTHOR(S) James L. Steiner and Donald A. Siebe

SUBMITTED TO L. M. Shotkin,
Division of Reactor System Safety
NL5650, Reactor Systems Branch
US Nuclear Regulatory Commission
Washington, DC 20555

DISCLAIMER

This report was prepared as an account of work sponsored by an agency of the United States Government. Neither the United States Government nor any agency thereof, nor any of their employees, makes any warranty, express or implied, or assumes any legal liability or responsibility for the accuracy, completeness, or usefulness of any information, apparatus, product, or process disclosed, or represents that its use would not infringe privately owned rights. Reference herein to any specific commercial product, process, or service by trade name, trademark, manufacturer, or otherwise does not necessarily constitute or imply its endorsement, recommendation, or favoring by the United States Government or any agency thereof. The views and opinions of authors expressed herein do not necessarily state or reflect those of the United States Government or any agency thereof.

This document contains information which is proprietary to the University of California. It is to be controlled and handled in accordance with the provisions of the University of California Policy on the Control and Handling of Proprietary Information.

This document is prepared for the use of the U.S. Nuclear Regulatory Commission. It is to be controlled and handled in accordance with the provisions of the U.S. Nuclear Regulatory Commission Policy on the Control and Handling of Proprietary Information.

MASTER

Los Alamos

Los Alamos National Laboratory
Los Alamos, New Mexico 87545

ONCE-THROUGH STEAM-GENERATOR SENSITIVITY CALCULATIONS*

by

James L. Steiner and Donald A. Siebe

Reactor Design and Analysis Group
Nuclear Technology and Engineering Division
Los Alamos National Laboratory
Los Alamos, New Mexico 87545

ABSTRACT

A series of TRAC-PF1/MOD2 thermal-hydraulic calculations has been performed to determine the effect of uncertainties in modeling once-through steam-generator (OTSG) secondary-side phenomena on the calculated behavior of Babcock & Wilcox power plants. The calculations were performed by varying parameters in correlations for the secondary-side phenomena. The parameters and transients were chosen to show the maximum expected sensitivity of the calculated results to the parameter variations. The parameters were then varied over a range representing the estimated uncertainty in the correlation. In this manner, the sensitivity of the calculated plant behavior to the modeling uncertainties was determined with a reasonable number of calculations. The sensitivity of calculated plant behavior to variations in interfacial heat-transfer in the OTSG secondaries was determined in a series of steam-generator overfill transient calculations. Calculations were performed for a main steam line break (MSLB) transient to quantify the sensitivity to variations in interfacial drag in the secondaries; the interfacial drag was varied in these calculations to indicate the effects of entrainment and de-entrainment processes, for which no specific models exist in the code. In addition to the transient calculations, a series of steady state calculations was performed to determine the sensitivity of the OTSG primary-to-secondary heat transfer to the assumed fraction of tubes wetted by the auxiliary feedwater (AFW) injection. The plant model used for the sensitivity calculations was qualified by performing a benchmark calculation for a natural circulation test in the TMI 1 plant.

The results of the plant transient calculations confirmed the expected sensitivity to the varied parameters and indicated a large sensitivity of the MSLB results to variations in the interfacial drag, whereas the sensitivity to interfacial heat transfer variations was very small in the steam generator overfill calculations. The steady state calculation

* This work was funded by the US Nuclear Regulatory Commission (NRC) Office of Nuclear Regulatory Research, Division of Accident Evaluation.

results showed that the condensation heat transfer during AFW boiler-condenser mode is nearly proportional to the assumed wetting fraction. Finally, the results of the benchmark calculation confirmed the ability of the TRAC-PF1/MOD2 code and input model to calculate the OTSG thermal center elevation for the conditions in the TMI-1 natural circulation test. The results provide information for determining whether additional experimental data are needed to improve the accuracy of calculated OTSG behavior. If additional experimental data for OTSG phenomena are needed, the results of the calculations indicate that data to characterize interfacial drag and entrainment/de-entrainment at the tube support plates are needed more than data for interfacial heat transfer or tube wetting.

SUMMARY

A study was performed to determine the impact of uncertainties in the modeling of once-through steam-generator (OTSG) secondary phenomena and processes on thermal-hydraulic system code calculations for plants with OTSGs. The study was a cooperative effort between the Idaho National Engineering Laboratory and Los Alamos National Laboratory to determine whether the results of safety calculations for nuclear power plants could be significantly affected by the OTSG modeling uncertainties, and to identify additional experimental data needs. The methodology used for the study was to review all phenomena and processes not fully characterized by existing correlations and identify the phenomena or processes most likely to impact plant transient calculations, along with the type of transient that would be most affected. Calculations were then performed with TRAC-PF1/MOD2 and RELAP5/MOD2 for the selected transients at the estimated extremes of the uncertainty in the phenomenon or process. This procedure identified the range of sensitivity of the calculated results to the modeling uncertainty by defining the bounds of the range.

The parameters varied in the plant transient sensitivity calculations were selected by reviewing all of the OTSG phenomena and processes and determining the phenomena or processes whose estimated uncertainties would have the greatest impact on the calculated results. In this procedure some of the phenomena and processes, such as flow-induced vibrations, were eliminated because they are not fully represented in thermal hydraulic code calculations. The sensitivity calculations were then performed by varying the parameters over a range representing the estimated uncertainty in the corresponding phenomenon or process. The parameters chosen for variation in the sensitivity calculations were the interfacial heat transfer between the liquid and vapor phases in the OTSG secondaries (subsequently referred to as phenomena HI10), and interfacial drag between liquid and vapor in the secondaries (subsequently referred to as phenomena HY3).

The transient calculations for the sensitivity study were chosen to show the maximum sensitivity to the varied parameters. Three calculations were performed for each transient including a nominal calculation with the nominal parameter value, and two calculations with the parameter values representing the extremes of the estimated uncertainty in the particular

phenomenon or process. In this manner the maximum sensitivity of calculated results to estimated uncertainties in the OTSG phenomena and processes was estimated with a reasonable number of plant calculations.

A steam-generator overfill transient was chosen to quantify the sensitivity to interfacial heat transfer in the OTSG secondaries. In an overfill transient, the OTSG secondaries are filled by excessive auxiliary feedwater (AFW) injection, during the overfill, the liquid in the secondaries is heated by the steam in the secondaries and also by contact with the tubes. The overfill transient was chosen because of the expected sensitivity of the secondary fluid temperatures and primary system cooldown rate to the interfacial heat transfer in the OTSG secondaries. Overfill sensitivity calculations were performed with both TRAC and RELAP; the varied parameter was the liquid-to-vapor heat-transfer coefficient in the OTSG secondaries.

A main steam line break (MSLB) transient was chosen to define the sensitivity to interfacial drag in the OTSG secondaries. In a MSLB transient, the affected OTSG secondary depressurizes and voids rapidly, during depressurization, the flow and void distribution in the secondary and heat removal from the primary depend strongly on the interfacial drag in the OTSG secondary. Therefore, the MSLB transient was expected to show the maximum sensitivity of the calculated behavior to variations in interfacial drag. The drag coefficient between liquid and vapor phases in the OTSG secondaries was the parameter varied in both the RELAP and TRAC MSLB sensitivity calculations.

In addition to the plant transient sensitivity calculations, a series of steady-state calculations was performed to determine the sensitivity of the OTSG primary to secondary heat transfer to the fraction of tubes wetted by AFW injection in the top of the secondaries. These "mapping sensitivity calculations" were performed with a series of assumed tube wetting fractions to map the OTSG performance as a function of wetting fraction. Two types of mapping sensitivity calculations were performed: natural circulation mapping calculations were performed using RELAP to determine the sensitivity of the OTSG thermal center elevation to the tube wetting fraction, and boiler-condenser mode (BCM) mapping calculations were performed using a model of a single OTSG with TRAC to determine the sensitivity of the condensation heat transfer in BCM to the wetting fraction.

The RELAP and TRAC models used for the OTSG sensitivity calculations were based on existing models of the Oconee plant. The models used the same nodalization for the OTSG primary and secondary regions and similar nodalizations for the loop piping and reactor vessel components. The 2-D calculation option in TRAC was used for the OTSG secondaries to provide a more accurate representation of the cross flows in the secondaries. The TRAC code and model used for the sensitivity calculations were qualified by performing a benchmark calculation for a natural circulation test in the Three Mile Island (TMI) plant and then comparing the results of the calculation to data from the test.

The results of the BCM mapping calculations show that high primary-to-secondary heat transfer rates are possible in BCM and that the BCM heat transfer rate increases almost linearly with the assumed wetting fraction. At the larger wetting fractions, however, the increase in heat transfer is slightly less than linear, which indicates that the heat transfer may be limited by one of the film coefficients adjacent to the tube surfaces rather than limited by the conduction capacity of the tubes. The sensitivity to wetting fraction indicate a need for data to characterize the AFW tube wetting profile. In plant calculations, however, the

condensation heat transfer during BCM reduces the vapor pressure inside the tubes, allowing liquid to rise in the tubes and thereby reducing the condensation surface area. The need for wetting profile data is thus diminished by this self-limiting/self-correcting characteristic of BCM in plant transients.

The results of the overfill sensitivity calculations show that with increased interfacial heat transfer, the secondary pool temperature was increased slightly and the primary depressurization rate was reduced. Conversely, when the interfacial heat transfer was reduced, the primary depressurization rate was increased as expected. The results of the overfill calculations both confirm the expected sensitivity to variations in the interfacial heat transfer and indicate that the magnitude of the sensitivity is very small.

The MSLB sensitivity calculation results show that when the interfacial drag is reduced, gravitational separation of liquid and vapor is increased in the OTSG secondaries. With increased phase separation, the AFW penetrates lower in the affected steam generator, resulting in a higher steam line void fraction and increased primary heat removal. The MSLB calculations show a large sensitivity of the calculated results to variations in the interfacial drag during blowdown of the steam generator in the affected loop. The primary effect of the drag variations was to alter the heat removal rate in the affected steam generator and the primary depressurization rate. The overall trends of the three MSLB calculations, however, were not affected by the drag variations, although the major events were shifted in time by the variations.

Comparison of the TMI natural circulation benchmark calculation to test data showed reasonable agreement between measured and calculated parameters. In particular, the calculated natural circulation flow rate was within the uncertainty of the measured flow rate. This indicates that the OTSG thermal center elevation and corresponding axial heat-transfer distribution were accurately calculated for the conditions in the TMI test. Additional experimental data for a wider range of conditions would permit a more complete qualification of the code and model used for the sensitivity calculations.

The results of the BCM mapping calculations indicate that data for defining the AFW tube wetting profile are of high importance for characterizing the BCM heat transfer. Experience with plant transient calculations, however, shows that BCM is self-correcting and highly dependent on phenomena elsewhere in the primary that affect the level in the OTSG tubes, such as the break flow in a loss-of-coolant accident. The results of the overfill and MSLB sensitivity calculations show that experimental data to characterize interfacial drag and the related entrainment/de-entrainment process at the tube support plates (for which no models exist) are needed more than data to characterize interfacial heat transfer.

I. INTRODUCTION

A wide range of physical phenomena and processes have been identified in Sec. 5 that can occur in the secondary sides of once through steam generators (OTSGs). Many of these phenomena and processes can be accurately characterized by correlations based on experimental data. The existing experimental data base, however, is not sufficient to fully quantify all of the phenomena and processes possible in the OTSG secondaries. Known limitations of the correlations for the secondary side phenomena, such as wall to liquid film heat transfer, lead to uncertainty in the results of thermal hydraulic system code predictions of nuclear power plant behavior under postulated abnormal operating conditions.

TABLE I
MAPPING SENSITIVITY CALCULATIONS

LANL	INEL
Eight AFW BCM mapping sensitivity calculations for 0.26, 0.787, 1, 5, 10, 25, 50, and 100% AFW wetting fractions.	Eight natural circulation mapping sensitivity calculations for 0, 0.26, 0.787, 1, 5, 10, 25, and 50% AFW wetting fractions.

A study was performed in the spring of 1988 to quantify the effects of OTSG modeling uncertainties on overall calculated plant behavior. The study was a cooperative effort between the Idaho National Engineering Laboratory (INEL) and Los Alamos National Laboratory (LANL) to determine whether the results of safety calculations for nuclear power plants could be significantly affected by the OTSG modeling uncertainties, and to identify additional experimental data needs. The methodology used for the study was to review all phenomena not fully characterized by existing correlations and select the phenomena most likely to impact plant transient calculations, along with the type of transient that would be most affected. The phenomena and transient selection was a joint effort between INEL, LANL, and the Technical Advisory Group (TAG). Calculations were then performed for the selected transients at the extremes of the correlation uncertainty. This procedure identified the range of sensitivity of the calculated results to the correlation uncertainty by defining the bounds of the range.

Steady-state and transient calculations for the sensitivity study were selected based on their expected sensitivity to the varied parameters. The steady-state calculations were chosen to quantify the steady-state sensitivity of the OTSG performance (as indicated by the primary-to-secondary heat transfer and thermal center elevation) during auxiliary feedwater (AFW) operation to the number of tubes wetted by the AFW. These "mapping sensitivity calculations" were performed with a series of assumed tube wetting fractions to map the OTSG performance as a function of wetting fraction. The mapping calculations performed for the sensitivity study are summarized in Table I. The boiler-condenser mode (BCM) mapping calculations were performed at LANL with TRAC-PF1/MOD2 using an OTSG model with driver components to maintain constant levels in the primary and secondary sides. The model was used to determine the condensation heat-transfer rate in BCM as a function of tube wetting fraction and level in the primary side of the OTSG. The natural circulation mapping calculations were performed at INEL with RELAP5/MOD2 using a full plant model. These calculations determined the steam generator thermal center elevation and corresponding primary system natural circulation flow during AFW operation as functions of the tube wetting fraction and secondary level.

The transient calculations for the sensitivity study (Table II) were chosen to show the maximum sensitivity to the varied parameters. A steam generator overflow transient was chosen to quantify the sensitivity to interfacial heat transfer in the OTSG secondaries. In an overflow transient, the OTSG secondaries are filled by excessive AFW injection. During the overflow, the

TABLE II
PLANT TRANSIENT SENSITIVITY CALCULATIONS

LANL	INEL
Nominal steam-generator (SG) overfill plant calculation, transient initiated by loss of offsite power.	Nominal SG overfill plant calculation, 10% wetting fraction, transient initiated by loss of offsite power.
SG overfill plant sensitivity calculation with 0.1 multiplier on interfacial heat transfer.	SG overfill plant sensitivity calculation with 0.1 multiplier on interfacial heat transfer.
SG overfill plant sensitivity calculation with multiplier of 3 on interfacial heat transfer.	SG overfill plant sensitivity calculation with multiplier of 3 on interfacial heat transfer.
	SG overfill plant sensitivity calculation with 3% wetting fraction, no multiplier on interfacial heat transfer.
Nominal MSLB plant calculation with break area = steam line area and pumps on.	Nominal MSLB plant calculation with break area = steam line area and pumps on.
Nominal MSLB plant calculation with break area = TBV area and pumps on.	
MSLB plant sensitivity calculation with 0.001 multiplier on interfacial drag in SG secondaries, pumps on, and TBV area.	MSLB plant sensitivity calculation with 0.001 multiplier on interfacial drag in SG secondaries, pumps on, and steam line area.
MSLB plant sensitivity calculation with 1000 multiplier on interfacial drag in SG secondaries, pumps on, and TBV area.	MSLB plant sensitivity calculation with 1000 multiplier on interfacial drag in SG secondaries, pumps on, and steam line area.
TMI plant benchmark calculation.	TMI plant benchmark calculation.

steam in the secondaries is cooled by the AFW liquid injected into the secondaries, and the axial fluid temperature distribution, therefore, depends on the interfacial heat-transfer rate. The overfill transient was chosen because of the expected sensitivity of the OTSG axial heat transfer distribution and primary system cooldown rate to the interfacial heat transfer in the OTSG secondaries. A series of steam generator overfill transient calculations was performed with TRAC PF1/MOD1 and RELAP5/MOD2 to determine the sensitivity to interfacial heat

transfer. These calculations included a nominal overfill transient and two additional calculations with multipliers of 0.1 and 3 applied to the interfacial heat-transfer coefficient between the liquid and vapor phases in the OTSG secondaries. These multiplier values have been determined to represent the extremes of the uncertainty in the interfacial heat transfer in a previous study related to the Upper Plenum Test Facility (Ref. 1). An additional overfill transient calculation was performed with RELAP5/MOD2 to determine whether the overfill calculation results were sensitive to the tube wetting fraction.

A main steam line break (MSLB) transient was chosen to define the sensitivity to interfacial drag in the OTSG secondaries. In a MSLB transient the affected OTSG secondary depressurizes and voids rapidly; during depressurization, the flow and void distribution in the secondary and heat removal from the primary depend strongly on the interfacial drag in the OTSG secondary. Therefore, the MSLB transient was expected to show the maximum sensitivity of the calculated behavior to variations in interfacial drag. RELAP5/MOD2 and TRAC-PF1/MOD2 were each used to perform a series of MSLB sensitivity calculations. In the RELAP5/MOD2 calculations the full steam line area was used for the MSLB area; the turbine bypass valve (TBV) area was used for the break area in the TRAC-PF1/MOD2 calculations to investigate the sensitivity at the lower end of the MSLB size spectrum. Each series of calculations included a nominal MSLB calculation and two additional calculations with multipliers of 0.001 and 1000 applied to the interfacial drag. This range of multipliers was chosen because the interfacial drag coefficient can vary over several orders of magnitude, depending on the flow regime, and as an estimate of the uncertainty in the entrainment/de-entrainment process at the tube support plates, for which no models exist. This procedure defined the sensitivity to interfacial drag over the range of steam line break sizes.

The model used for the OTSG sensitivity calculations was based on an existing model of the Oconee plant. The model was qualified by running a benchmark calculation for a natural circulation test conducted during startup of the TMI-1 plant, and comparing the calculated and observed OTSG performance. This report describes the model and calculations performed for the OTSG sensitivity study, the results of the calculations, and conclusions drawn from the results, and provides recommendations for future thermal-hydraulic testing to characterize OTSG phenomena.

II. MODEL DESCRIPTION

The primary piping and components were based on a TRAC-PF1/MOD1 (Refs. 2-4) model of the Oconee-1 plant that had been used for a Nuclear Regulatory Commission (NRC)-sponsored pressurized-thermal-shock study (Ref. 5). This model was later updated to create a TRAC-PF1/MOD2 model.

The steam generators were modeled with two PIPE components on the primary side of each. Two channels made from PIPE and TEE components were used to represent each steam generator secondary. One channel of the secondary and one of the PIPE components in the primary represented the portion of the steam generator and steam-generator tubes wetted by AFW flow. The other secondary channel and primary PIPE component represented the portion of a steam generator and steam-generator tubes that were not wetted by the AFW. The apportioning of wet and dry areas was made based on guidelines provided by Babcock & Wilcox (B&W) (Ref. 6).

A similarly noded model was used for pretest calculations for the Multi-Loop Integral System Test (MIST) facility. When MIST data became available, we found that this model predicted the steam-generator thermal center at too low an elevation in the steam-generator. This caused steady-state natural circulation flows to be underpredicted and primary pressure and hot-leg temperatures to be overpredicted (Ref. 7). In a study to determine model and code changes that would produce an adequate steady-state for MIST posttest calculations, we found that the two-channel secondary model did not allow sufficient steam flow between the channels. Noding and code changes were made so that a single channel could be used for the steam-generator secondary with two sets of heat transfer coefficients calculated, one for the nominally wet tubes and one for the nominally dry channel. We also found that determining the heat-transfer coefficients by redistributing liquid in the upper part of the steam generator from the nominally dry region to the nominally wet region and then multiplying the heat-transfer coefficient by a factor of 1.8 for the nominally wet portion of the steam generator produced an adequate steady state. A model used by B&W makes similar changes for modeling the MIST steam generators.

A developmental code version, TRAC-PF1/MOD2, has the capability to utilize a more physically correct model for the steam-generator secondaries. The 3-D VESSEL components can be used to model the steam-generator secondaries with generalized heat structures used to model heat-transfer paths. This capability was demonstrated earlier with a standalone model that used 25 cross-sectional nodes and 19 axial levels in a detailed model of a 19-tube MIST steam generator (Ref. 7). Since this capability produces a more realistic steam-generator model, we decided to utilize it for these sensitivity calculations.

A steam-generator model was developed using a 3-D VESSEL to represent the steam-generator secondaries. Three radial rings are used: the inner represents the nominally dry portion of the steam generator, the middle ring represents the nominally wetted portion of the steam generator, and the outer ring represents the downcomer and steam annulus. A cell theta dimension of 360° was used so the model is actually two dimensional. An 11-level axial noding was chosen to be consistent with noding in the model used by INEL.

Table III lists the hydrodynamic components by number, description, type, and number of cells. There are 62 hydrodynamic components, 210 3-D fluid cells, and 228 1-D fluid cells. Figure 1 shows the noding of the reactor vessel, Fig. 2 steam generator A, Fig. 3 the A-loop.

III RESULTS

The results of the mapping, overfill, and MSLB sensitivity calculations, and Three Mile Island (TMI) benchmark calculation performed with TRAC-PF1/MOD2 are described in the following subsections. For the BCM mapping calculations, the results define the BCM heat transfer as a function of the tube wetting fraction and level in the primary side of the OTSG. The results of the sensitivity calculations quantify the sensitivity of the calculated plant behavior to the varied parameters. The calculated results provide a basis for determining the importance of correlations for the varied parameters by defining the sensitivity of key calculated variables such as primary system pressure and primary cooldown rate.

A. AFW BCM Mapping Sensitivity Calculations

BCM describes a OTSG condition with condensation occurring in the primary side of the tubes at an elevation where there is liquid contact with the secondary side of the tubes

TABLE III
TRAC-PF1/MOD2 PLANT MODEL COMPONENT DESCRIPTIONS

Component No.	Description	Component Type	Number of Cells
1	Reactor vessel	VESSEL	12 x 2 x 6
11	Rod guide tube 1	PIPE	4
12	Rod guide tube 2	PIPE	4
13	Rod guide tube 3	PIPE	4
14	Rod guide tube 4	PIPE	4
15	Rod guide tube 5	PIPE	4
16	Rod guide tube 6	PIPE	4
80	Accumulator-a connection	PIPE	1
90	Accumulator-b connection	PIPE	1
81	Accumulator zero fill	FILL	1
91	Accumulator zero fill	FILL	1
50	Pressurizer	PRIZER	6
60	Pressurizer PORV	VALVE	1
70	PORV boundary	BREAK	1
100	A hot leg	TEE	20
102	A hot-leg to OTSG connection	PIPE	2
103	A OTSG primary inlet plenum	PLENUM	1
105	A OTSG wetted primary tube bundle	PIPE	13
104	A OTSG dry primary tube bundle	PIPE	13
106	A OTSG primary outlet plenum	PLENUM	1
108	A loop seal	TEE	10
130	A OTSG secondary shell	VESSEL	11 x 3 x 1
184	A AFW nozzle and line	PIPE	1
144	A steam line	PIPE	1
190	A main feedwater line	PIPE	1
110	A1 reactor coolant pump	PUMP	2
120	A2 reactor coolant pump	PUMP	2
112	A1 cold leg	TEE	9
122	A2 cold leg	TEE	9
114	A1 HPI	FILL	1
124	A2 HPI	FILL	1
146	A OTSG steam line	TEE	7
148	A turbine stop valve	VALVE	1
150	A steam line boundary	BREAK	1
152	A steam line SRV fill	FILL	1
185	A AFW fill	FILL	1

TABLE III Cont.
TRAC-PF1/MOD2 PLANT MODEL COMPONENT DESCRIPTIONS

Component No.	Description	Component Type	Number of Cells
188	A MFW fill	FILL	1
200	B hot leg	PIPE	12
202	B hot-leg to OTSG connection	PIPE	2
203	B OTSG primary inlet plenum	PLENUM	1
205	B OTSG wetted primary tube bundle	PIPE	13
204	B OTSG dry primary tube bundle	PIPE	13
206	B OTSG primary outlet plenum	PLENUM	1
208	B loop seal	TEE	10
230	B OTSG secondary shell	VESSEL	11 x 3 x 1
284	B AFW nozzle and line	PIPE	1
244	B steam line	PIPE	1
290	B main feedwater line	PIPE	1
210	B1 reactor coolant pump	PUMP	2
220	B2 reactor coolant pump	PUMP	2
212	B1 cold leg	TEE	9
222	B2 cold leg	TEE	3
226	B2 cold leg with leak site	TEE	7
228	Small break boundary	FILL	1
214	B1 HPI	FILL	1
224	B2 HPI	FILL	1
246	B OTSG steam line	TEE	7
248	B turbine stop valve	VALVE	1
250	B OTSG steam line boundary	BREAK	1
252	B OTSG steam line SRV fill	FILL	1
285	B AFW	FILL	1
288	B MFW	FILL	1

In BCM, the heat-transfer coefficient is high on both sides of the tubes and the primary-to-secondary heat-transfer rate is limited by the heat conduction capacity of the tubes. AFW BCM occurs in an OTSG when the AFW is active and the water level in the primary side of the tubes is below the AFW injection elevation. In AFW BCM, the tube surfaces wetted by AFW in the secondary are adjacent to higher temperature vapor inside the tubes. The heat-transfer rate in the AFW BCM depends on the surface area available for condensation, which is determined by the AFW wetting fraction and the primary level.

Eight BCM mapping sensitivity calculations were performed for 0.26, 0.787, 1, 5, 10, 25, 50, and 100% tube wetting fractions. Each calculation was a series of steady-state calculations

REACTOR VESSEL NODING ($r=2$, $z=12$, $\theta=6$)

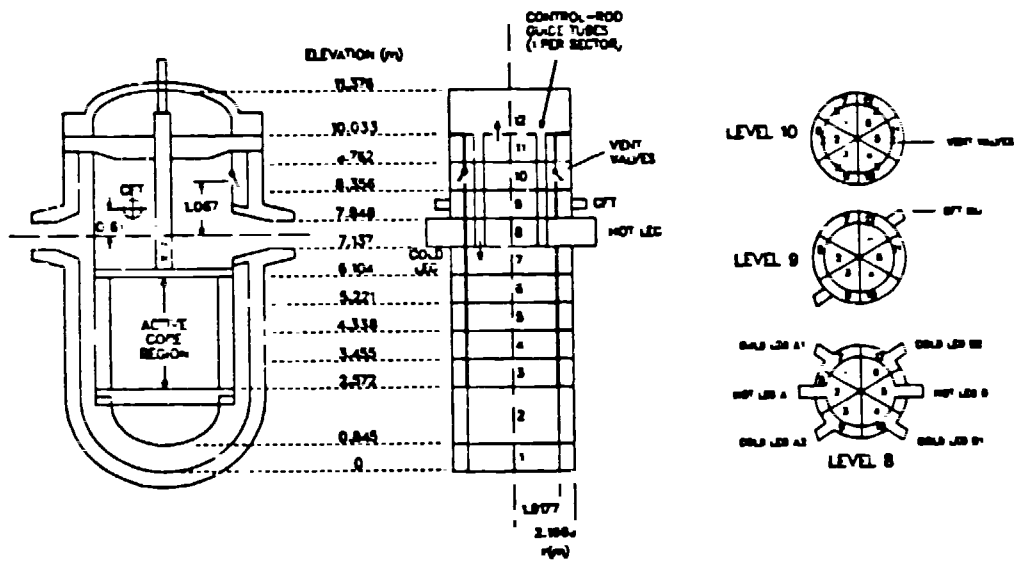


Fig. 1.
Reactor vessel nodalization

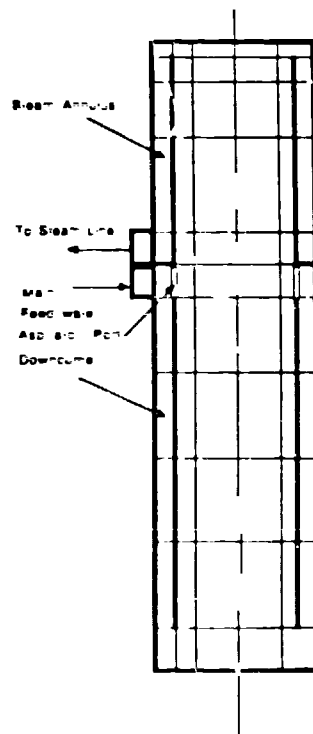


Fig. 2.
A loop steam generator nodalization

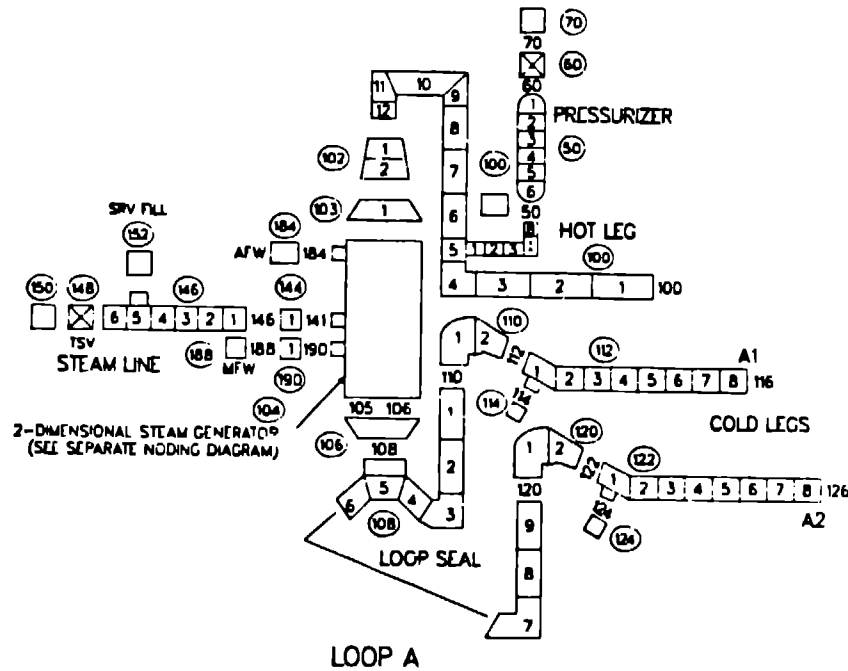


Fig. 3.
A-loop nodalization.

at different OTSG primary levels. The calculated total primary-to-secondary heat transfer from the BCM mapping calculations is shown as a function of the wetting fraction and primary level in Fig. 4. The BCM mapping calculations were performed with the primary pressure maintained at 11.99 MPa (1739 psia) and the secondary pressure maintained at 6.99 MPa (1014 psia); these are typical pressure values during periods of BCM in plant transient predictions. At these conditions, the results of the mapping calculations indicate that the BCM condensation heat transfer is approximately 75 - 85% of the total primary-to-secondary heat transfer. The remainder of the heat transfer results from steam cooling of tube surfaces not wetted by the AFW and from heat transfer below the secondary pool.

The results of the BCM mapping calculations show that high primary-to-secondary heat-transfer rates are possible in BCM and that the steam generators can remove a significant fraction of the core power during BCM. Fig. 4 also shows that the BCM heat-transfer rate increases almost linearly with wetting fraction. At the larger wetting fractions, however, the increase in heat transfer is slightly less than linear, indicating that the heat transfer may be limited by one of the film coefficients adjacent to the tube surfaces rather than limited by the conduction capacity of the tubes.

The results of the BCM mapping calculations demonstrate the strong sensitivity of the calculated BCM heat transfer to the assumed wetting fraction and level maintained in the primary side of the tubes. In plant calculations, however, the sensitivity to wetting fraction is greatly reduced because the primary levels are affected by the BCM heat transfer. The condensation heat transfer during BCM reduces the pressure of the vapor inside the steam generator tubes, allowing the liquid to rise in the tubes, thus reducing the surface area available

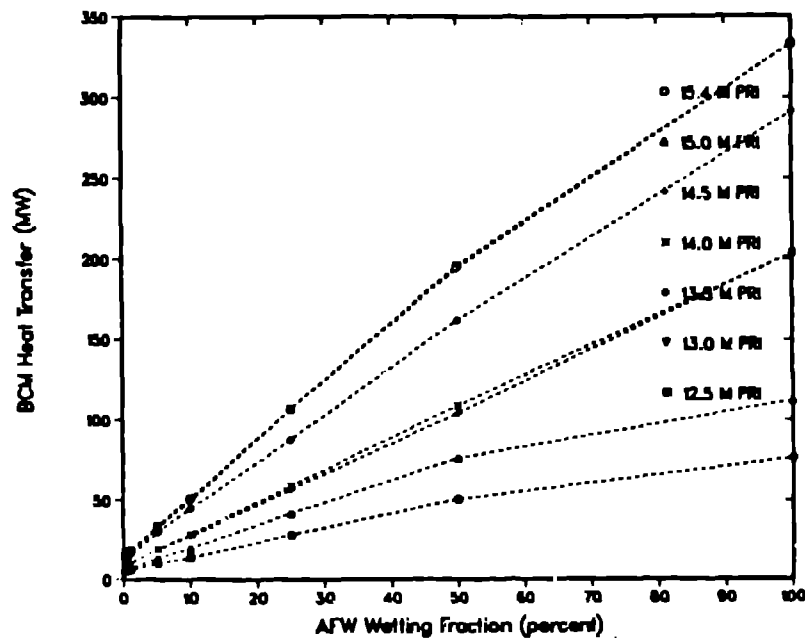


Fig. 4.

AFW BCM steam-generator heat transfer vs wetting fraction.

for condensation. The sensitivity of BCM effects to wetting fraction in plant calculations, therefore, is largely offset by the self-limiting nature of BCM.

B. Steam-Generator Overfill Sensitivity Calculations

A steam-generator overfill transient was chosen to demonstrate the sensitivity of calculated results to variations in liquid-vapor interfacial heat transfer in the steam-generator secondaries. The overfill sensitivity calculations were assumed to be initiated by a loss of offsite power with a subsequent failure of the secondary high-level limit signals. In this transient, the steam generator secondaries are overfilled by the AFW and the primary is cooled by natural circulation. During the overfill process, some of the vapor in the secondaries is condensed by the AFW while the remaining vapor is compressed by the rising secondary liquid level. The temperature of the liquid pool in the secondaries and corresponding primary heat removal rate during the overfill depends on the interfacial heat transfer in the secondaries. Results calculated for an overfill transient, therefore, are expected to be sensitive to variations in interfacial heat transfer in the secondaries.

Three steam generator overfill calculations were performed to determine the sensitivity of the calculated results to variations in interfacial heat transfer. The three calculations included a base case with no changes to the heat transfer coefficient and two sensitivity calculations, one with a multiplier of 3 and one with a multiplier of 0.1 applied to the interfacial heat transfer in the steam generator secondaries. A wetting fraction of 10% was used for each calculation

TABLE IV
STEAM-GENERATOR OVERFILL CALCULATION CONTROLS

Core power	Steady state:	2568 MW
	Transient:	Switch to power vs time curve at beginning of transient
Main feedwater	Steady state:	Vary main feed to maintain secondary boiler section level at 5.5283 ft
	Transient:	Ramp steady-state flow to zero in the first 5 s of the transient
AFW flow	Steady state:	Off
	Transient:	Use AFW flow vs secondary pressure, do not shutoff on high level, 5 s delay to simulate main feedwater pump coastdown at beginning of transient
Steam flow	Steam line connected in series to VALVE and BREAK component (pressure boundary condition: same as TMDPVOL in RELAP5)	
	Steady state:	Constant BREAK pressure = 917 psia; VALVE open
	Transient:	Atmospheric BREAK pressure; VALVE starts to open at 1025 psia, full open at 1085 psia
HPI	Actuate at 1515 psia, do not throttle or terminate	
PORV	Open at 2465 psia, close at 2415 psia	
Core flood tank	Deactivated (won't open in this transient)	
Primary pumps	Steady state:	Constant speed = 154.18 rad/s
	Transient:	Freewheel
Pressurizer heaters	Off during transient	
Terminate calculation	When secondaries full (approximately 1000 s)	

and the calculations were terminated at 1000 s when the secondaries were liquid full. The controls used for the overfill calculations are summarized in Table IV.

At the start of the steam generator overfill calculations, the reactor and primary coolant pumps were tripped, and the ISVs were assumed to close in 5 s. During the first 5 s of the overfill calculations, the primary and secondaries depressurized rapidly (Fig. 5) while the ISVs were closing. After 5 s the secondary pressures recovered to the IBV set point of

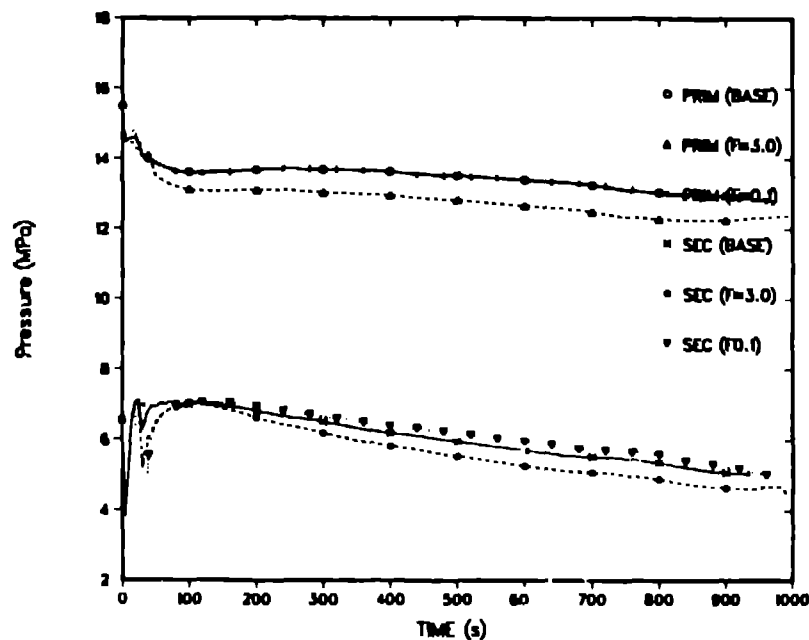


Fig. 5.

Primary and A-loop secondary pressures for overfill calculations.

7.07 MPa (1025 psia) and the TBVs opened, causing the secondary pressures to decrease at about 60 s as shown in Fig. 5. Shortly after this time the TBVs closed on low secondary pressure and remained closed in all three overfill calculations. After the TBVs closed, Fig. 5 shows that the secondary pressures recovered to just below the TBV set point at 100 s and then gradually decreased for the remainder of the calculations. During the secondary pressure recovery from 60 to 100 s, heat was removed from the primaries and the primary pressures in Fig. 5 decreased.

After the TBVs closed at 60 s, the secondary pressurization rate in the overfill calculations depended on the interfacial heat transfer multiplier. With a multiplier of 3, steam condensed more rapidly on the AFW injected in the top of the secondaries, and the secondary pressurization was slower. The slower pressurization with the multiplier of 3 resulted in more flashing in the secondary pools and more primary heat removal. As a result, the primary pressure decreased more from 60 to 100 s in Fig. 5 with the multiplier of 3. After 100 s, the heat removal rate during the steam generator overfill was approximately equal to the core power and the primary and secondary pressures stabilized in all three overfill calculations. The overfill rate was slightly higher with the multiplier of 3 because in this case there was more steam condensation on the AFW which reduced the secondary pressure (Fig. 5) and allowed a higher AFW injection rate.

The results of the overfill calculations confirm the expected sensitivity to variations in the interfacial heat transfer for this type of transient and indicate that the magnitude of the sensitivity is very small. In addition, neither the power operated relief valve (PORV) set point of 17.00 MPa (2465 psia) nor the high pressure injection (HPI) set point of 10.45 MPa

(1515 psia) were approached in the calculations. If either of these set points had been reached because of a variation in the interfacial heat transfer, the sensitivity of the results would have been greatly increased. At the end of the overfill calculations, the secondaries were liquid full and the primary was in stable natural circulation. If the calculations were extended further, this situation would be expected to continue with subsequent TBV openings to remove decay heat and minor changes in the primary and secondary pressures.

C. MSLB Sensitivity Calculations

A MSLB transient was selected to show the maximum sensitivity of calculated results to variations in the interfacial drag in the steam-generator secondaries. The interfacial drag variations represent the uncertainty in the entrainment/de-entrainment process at the tube support plates. In a MSLB transient, the steam generator affected by the steam line break depressurizes rapidly and eventually loses all of its liquid inventory. During depressurization the flow and void distributions and primary heat removal rate in the affected steam-generator secondary are highly dependent on the interfacial drag. The calculated primary and secondary responses are therefore very sensitive to interfacial drag in a MSLB transient.

The MSLB calculations performed with TRAC-PF1/MOD2 assumed a steam line break area equal to the TBV area (approximately 3% of full steam line area). The three MSLB sensitivity calculations performed with TRAC-PF1/MOD2 were a base case with no interfacial drag changes and two sensitivity calculations, one with a multiplier of 0.001 and one with a multiplier of 1000 applied to the drag. A wetting fraction of 10% was used for each of the calculations and the calculations were terminated well after the period of steam-generator blowdown and primary cooldown. The controls for the MSLB sensitivity calculations are shown in Table V.

At the beginning of the MSLB calculations, the reactor power decay was started and the TSVs were assumed to close in 5 s. Figure 6 shows that the primary and secondary pressures decreased rapidly during the 5-s TSV closure period at the beginning of the base case MSLB calculation. After the TSV was fully closed, the secondary pressures recovered and the primary continued to depressurize at a lower rate.

The A-loop (affected loop) steam generator depressurized after 20 s, because of the steam line break, until approximately 100 s when the steam flow decreased to the AFW flow in this loop (Fig. 7). After this time the A loop steam generator pressure remained stable until 300 s when the AFW was assumed to be terminated by an operator action. The A loop steam generator then depressurized to near atmospheric pressure in the absence of AFW injection (Fig. 6).

The B loop steam generator pressure in Fig. 6 recovered to 5.3 MPa (769 psia) after the TSV closure at 5 s and then gradually decreased because of the cooling effects of the AFW injection. At approximately 250 s, the B loop steam generator was nearly refilled to the 6.10 m (20 ft) high level set point and the AFW flow began to decrease (Fig. 8). With the reduced AFW flow, the B loop steam generator pressure decreased at a reduced rate after 250 s, reaching a minimum value of 4.7 MPa (682 psia) at 320 s. After 320 s, Fig. 8 shows that there was very little AFW flow in the B loop steam generator and the secondary pressure in Fig. 6 increased for the remainder of the calculation.

The primary pressure in the MSLB base case calculation was governed mainly by the heat removal in the A loop (affected loop) steam generator. The primary depressurized steadily

TABLE V
MSLB CALCULATION CONTROLS

	A loop = affected loop for steam line break B loop = unaffected loop	
Core power	Steady state:	2568 MW
	Transient:	Switch to power vs time curve (MIST power decay curve) at beginning of transient
Main feedwater	Steady state:	Vary main feed to maintain secondary boiler section level at 5.5283 ft
	Transient:	Off
AFW flow	Steady state:	Off
	Transient:	Vary AFW to maintain secondary boiler section level at 20 ft. terminate AFW at 5 min
Steam flow	Steam line connected in series to VALVE and BREAK component (pressure boundary condition: same as TMDPVOL in RELAP5)	
	Steady state:	Constant BREAK pressure = 917 psia; VALVE open
	Transient:	Atmospheric BREAK pressure: VALVE remains open
	(A loop)	
	Transient:	Atmospheric BREAK pressure. VALVE closes in
	(B loop)	0.4 s after beginning of transient, then starts to open at 1025 psia, full open at 1085 psia
HPI	Actuate at 1515 psia, do not throttle or terminate	
PORV	Open at 2465 psia, close at 2415 psia	
CFT	Deactivated (won't open in this transient)	
Primary pumps	Steady state	Constant speed - 138.23 rad/s
	Transient:	Constant speed - 138.23 rad/s
Pressurizer heaters	On when pressure below 1975 psia	
Terminate calculation	When secondaries full (approximately 1000 s)	

during the first 300 s of the calculation when the AFW was active in the A loop. At 300 s the A loop AFW was terminated by operator action and the primary pressure in Fig. 6 then increased until 840 s when the pressurizer pressure reached the 17 MPa (2465 psia) PORV set point. The primary depressurization rate and minimum pressure of 11.1 MPa (1610 psia)

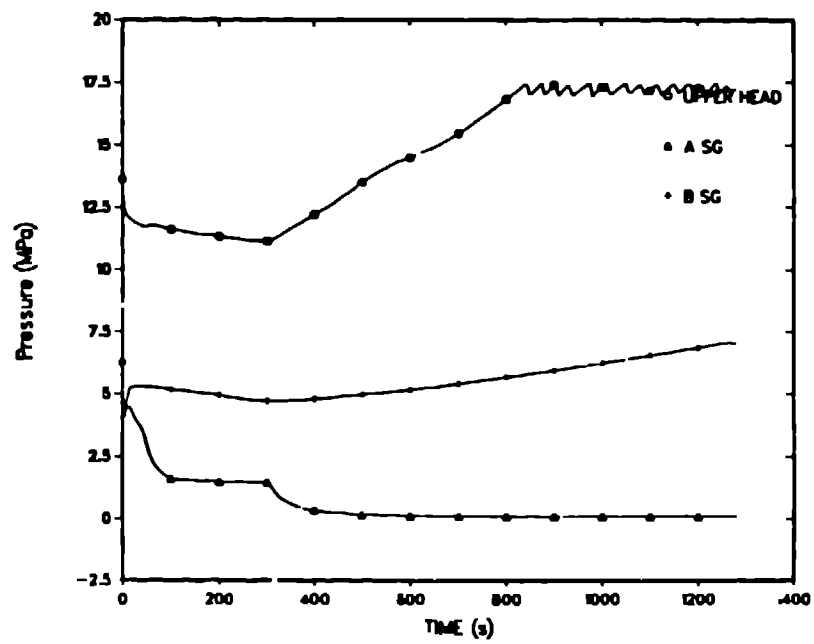


Fig. 6.
Primary and secondary pressures for MSLB base case

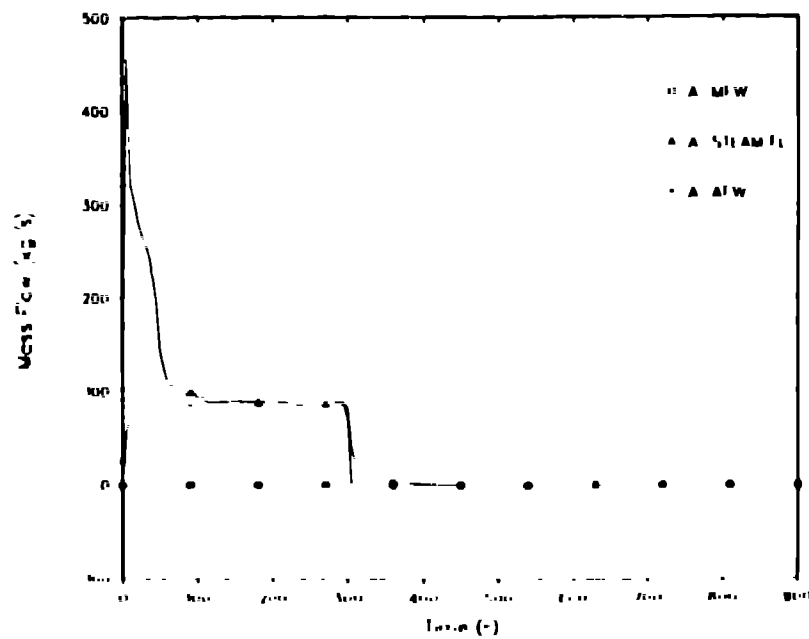


Fig. 7.
A loop steam generator flows for MSLB base case

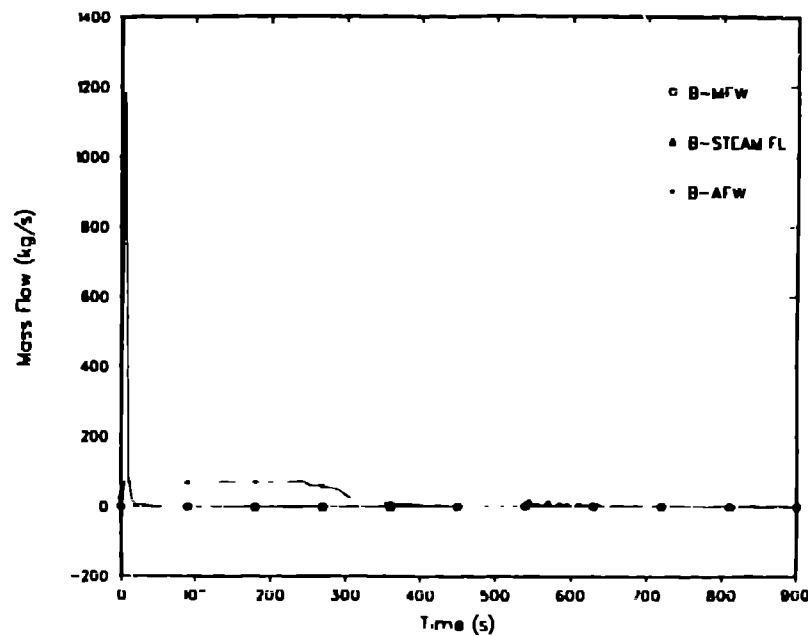


Fig. 8.
B-loop steam-generator flows for MSLB base case.

at 300 s in the MSLB base case calculation were determined by the magnitude of the primary-to secondary heat-transfer rate in the A-loop; these are the parameters that are sensitive to variations in the interfacial drag in the OTSG secondaries

The MSLB sensitivity calculation results show that when the interfacial drag is reduced, gravitational separation of liquid and vapor is increased in the OTSG secondaries. With increased phase separation, the AFW penetrates lower in the affected steam generator, resulting in a higher steam line void fraction (Fig. 9) and increased primary heat removal. Figures 10 and 11 show that during the 0 to 300 s period when the AFW was active in the affected loop (A loop) steam generator, the primary depressurization rate was markedly increased when a 0.001 multiplier was used for the interfacial drag, and reduced slightly when a value of 1000 was used for the multiplier. Comparison of Figs. 6-11 also shows that the overall trends of the MSLB sensitivity calculations were similar although the HPI was activated at 85 s when the 0.001 multiplier was used (Fig. 10) because of the lower primary pressure calculated.

The primary repressurized steadily after 300 s in the MSLB calculations when AFW was terminated in the A loop; results of the calculations show that the repressurization rate was sensitive to the interfacial drag. After 300 s the AFW remained active in the B loop until the B loop steam generator secondary was filled to the 6.10 m (20 ft) high level set point. The primary repressurization rate was increased during this period when the interfacial drag was reduced (Figs. 6-11). With less drag and more separation in the B loop secondary, the void fraction was higher above the pool in the B loop secondary and the heat transfer above the pool was reduced. The reduced heat transfer resulted in the higher primary repressurization rate after 300 s with the 0.001 drag multiplier. The primary repressurized to the 17.00 MPa

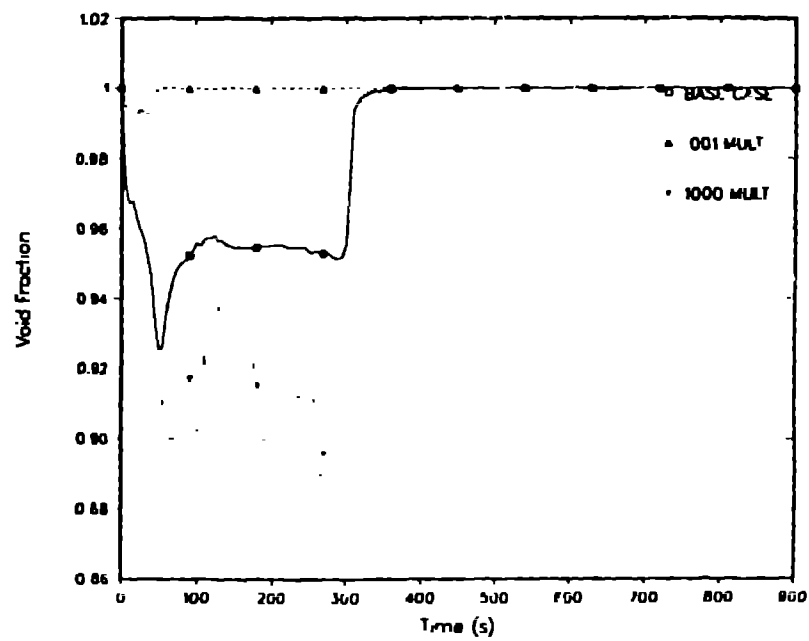


Fig. 9.
A-loop steam line void fraction for MSLB calculations.

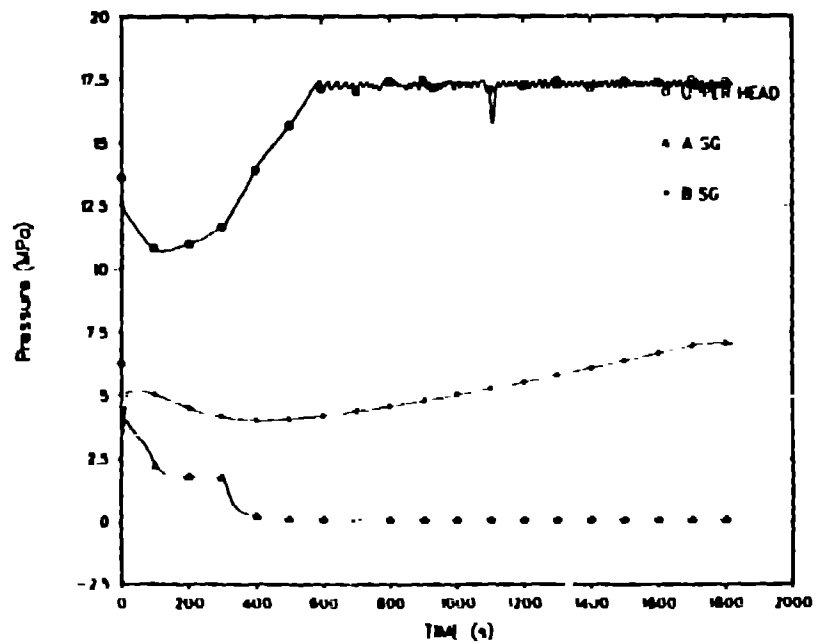


Fig. 10.
Primary and secondary pressures for 0.001 multiplier MSLB calculation.

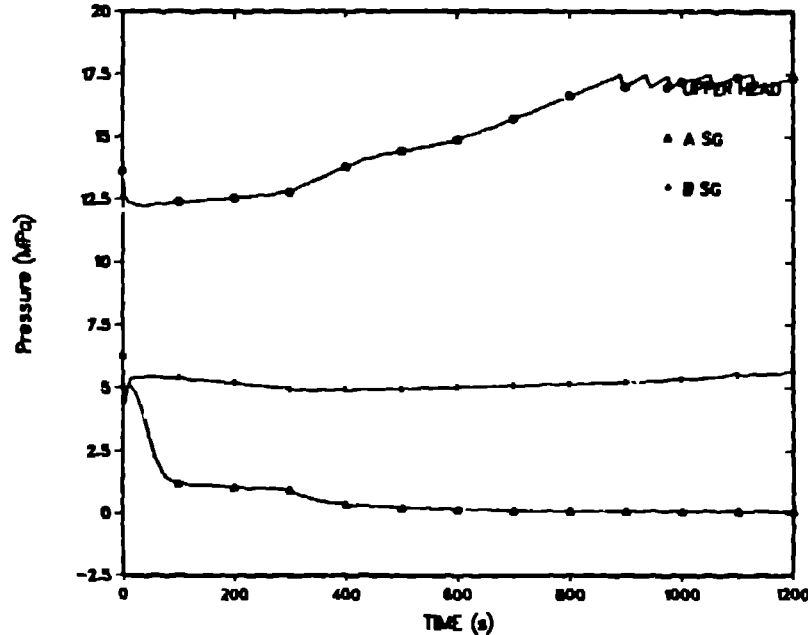


Fig. 11.

Primary and secondary pressures for 1000 multiplier MSLB calculation.

(2465-psia) PORV set point in each of the MSLB calculations; Figs. 6-11 show that the time to PORV actuation was increased when the drag was increased.

The MSLB calculations show a large sensitivity of the calculated results to variations in the interfacial drag during blowdown of the affected loop steam generator. The primary effect of the drag variations was to alter the heat removal rate in the affected steam generator and the primary depressurization rate. The overall trends of the three MSLB calculations were not affected by the drag variations, although the major events were shifted in time by the variations. The primary and secondary conditions at the end of the MSLB calculations were the same: the affected steam generator was voided and depressurized, the unaffected steam generator was refilled to the high-level set point, and the primary pressure was controlled at the PORV set point.

D. TMI Benchmark Calculation

The TRAC-PF1/MOD2 code and model used for the sensitivity calculations were qualified by performing a benchmark calculation for a natural circulation test in the TMI plant. In the test, the reactor coolant pumps (RCPs) were not powered and the natural circulation flow rate in the primary system was determined by the OTSG thermal center elevation. Comparison of the observed and calculated natural circulation flow rate therefore provides a measure of the accuracy of the calculated OTSG behavior.

The TMI natural circulation test was initiated with the core power at 3.2% (81.2 MW), the RCPs running at full speed, and the OTSG secondary levels maintained at 6.3 m (20.6 ft) by the AFW in each loop. The test was started by tripping the RCPs, during the test the

core power was held at approximately 3.1%, the AFW flow was nearly constant in each loop, and the OTSG secondary pressures were maintained by using the TBVs to control the steam flow.

The TRAC-PF1/MOD2 calculation for the natural circulation test was run using data from the test for the boundary conditions. Measured core power data were available until 900 s after the RCPs were tripped, and were specified for the power in the calculation. For the remainder of the calculation, the power was assumed to be a constant equal to the measured power at 900 s. The measured OTSG secondary pressures were specified as pressure boundary conditions and the AFW flows in the calculation were set to the measured values in each loop. In the test, the pressurizer heaters were controlled based on pressurizer pressure; the same procedure was used in the calculation to control the pressurizer heaters based on the calculated pressurizer pressure. The calculation was started by tripping the RCPs to allow the pump rotors to freewheel. The TMI benchmark calculation controls are summarized in Table VI.

The measured data available from the TMI natural circulation test included the primary and secondary pressures, hot- and cold-leg temperatures, OTSG secondary and pressurizer levels, core power, hot-leg flow rate, and TBV stem position. Comparison of corresponding parameters from the benchmark calculation showed reasonable agreement with the measured values. The primary and secondary pressures from the calculation compared closely to the measured values (Fig. 12) since the primary pressure was controlled by the pressurizer heaters in both the test and the calculation, and the measured secondary pressures were specified as boundary conditions in the calculation.

The calculated natural circulation flow in the primary system also compared closely with data from the test. Figure 13 shows the total calculated loop flow, the total loop flow from the hot-leg flow measurements during the test, and the total loop flow determined from a core energy balance using the measured power and fluid temperatures in the hot and cold legs. The difference in the two total loop flows determined from test data is a result of the uncertainty in the hot-leg flow and core power measurements. Figure 13 shows excellent agreement between the calculated and measured natural circulation flow rates and also indicates that the calculated natural circulation flow rate may be at the high end of the uncertainty in the measured natural circulation flow rate after completion of the pump coastdown at 800 s.

The most significant difference between the benchmark calculation and the test occurred in the hot-leg temperatures. Figure 14 shows that, before 800 s, the calculated hot-leg temperatures exceeded the test data and, after 800 s, the calculated hot-leg temperatures were slightly below the data. This difference is consistent with the differences in the total loop flows shown in Fig. 13. Prior to the completion of the reactor coolant pump coastdown at approximately 800 s, Fig. 13 indicates that the calculated natural circulation flow was below the natural circulation flow in the test. As a result, the fluid transit time through the core was increased in the calculation and the calculated hot-leg temperatures exceeded the test data until 800 s. After 800 s the situation was reversed: the calculated natural circulation flow exceeded the measured flow (Fig. 13), resulting in lower calculated hot-leg temperatures as compared to the measured values (Fig. 14). At the end of the test at 1800 s, Fig. 13 shows that the calculated natural circulation flow matched the upper measured flow of 670 kg/s while the lower measured value was 410 kg/s. Assuming a core power of 3.1% (78.7 MW), an energy balance shows that if the calculated natural circulation flow had been midway between the

TABLE VI
TMI BENCHMARK CALCULATION CONTROLS

Core power	Steady state:	81.2 MW
	Transient:	Switch to measured power vs time curve at beginning of transient
Main	Steady state:	Off
	Transient:	Off
AFW flow	Steady state:	Vary AFW to maintain secondary levels at 20.6 ft
	Transient:	Use measured AFW flow
Steam flow	Steam line connected in series to VALVE and BREAK component (pressure boundary condition: same as TMDPVOL in RELAP5)	
	Steady state:	Constant BREAK pressure = 953 psia: (A loop). 959 psia (B loop); VALVE open
	Transient:	Measured pressures in A and B loop BREAKS: VALVES open
HPI	Deactivated	
PORV	Deactivated	
CFT	Deactivated	
Primary pumps	Steady state:	Constant speed = 154.18 rad/s
	Transient:	Freewheel
Pressurizer heaters	On when pressure below 2135 psia during transient	
Terminate calculation	At 1800 s (end of test)	

two measured values, then the calculated hot-leg temperature in Fig. 14 would have matched the measured value of 580 K at 1800 s.

In both the test and the calculation, the cold-leg temperatures (Fig. 15) remained within 1.5 K of the OTSG secondary saturation temperatures after 100 s when the pump coastdown was 90% complete (Fig. 13). The overall comparison of the loop flows and hot- and cold-leg fluid temperatures in Figs. 13–15 was reasonable: differences between the measured and calculated parameters were small and the same trends occurred in the calculation as in the test.

The differences in the measured and calculated hot leg temperatures in Fig. 14 were probably caused by uncertainty in modeling the low speed TMI pump performance and the core power during the natural circulation test. The homologous curves in the TRAC PF1/MOD2

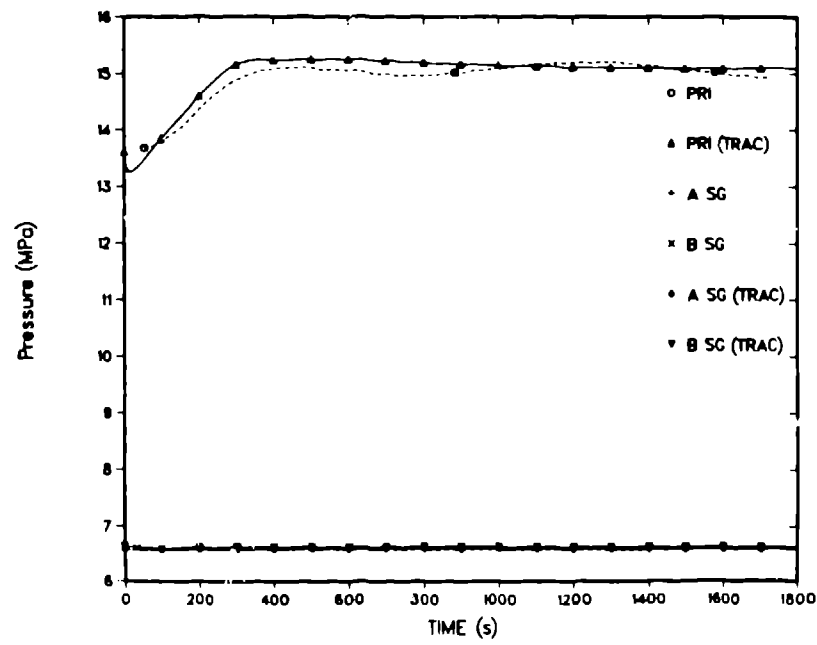


Fig. 12.
Primary and secondary pressures for TMI natural circulation test.

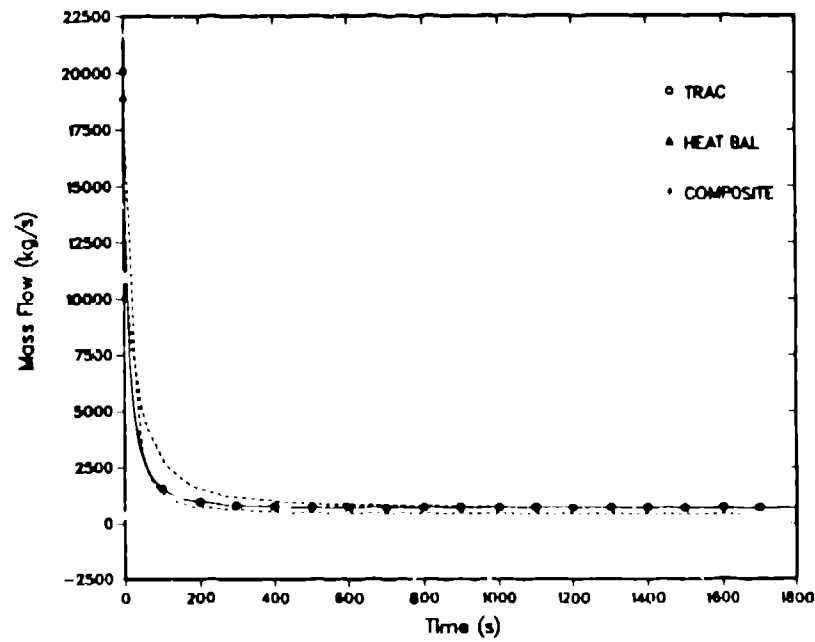


Fig. 13.
Total loop flow for TMI natural circulation tests.

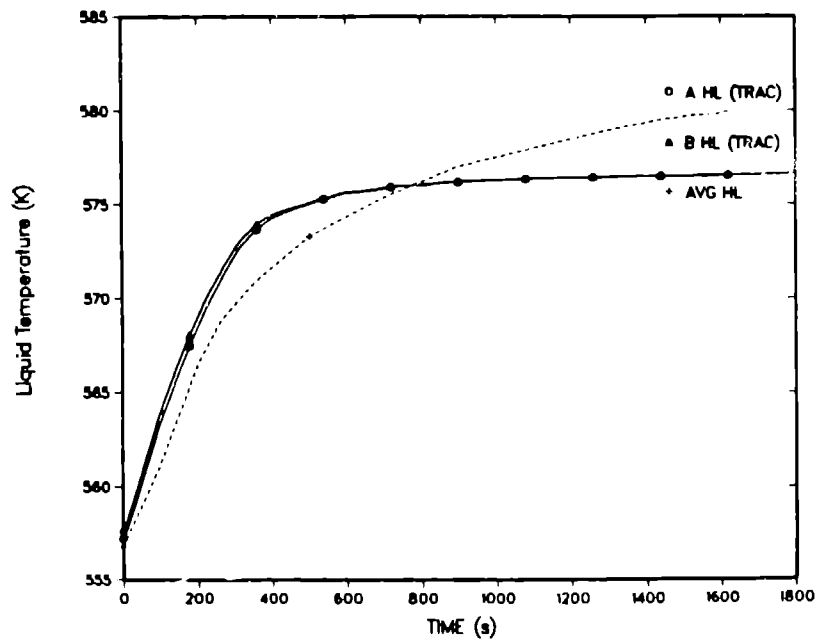


Fig. 14.
Hot-leg temperatures for TMI natural circulation test.

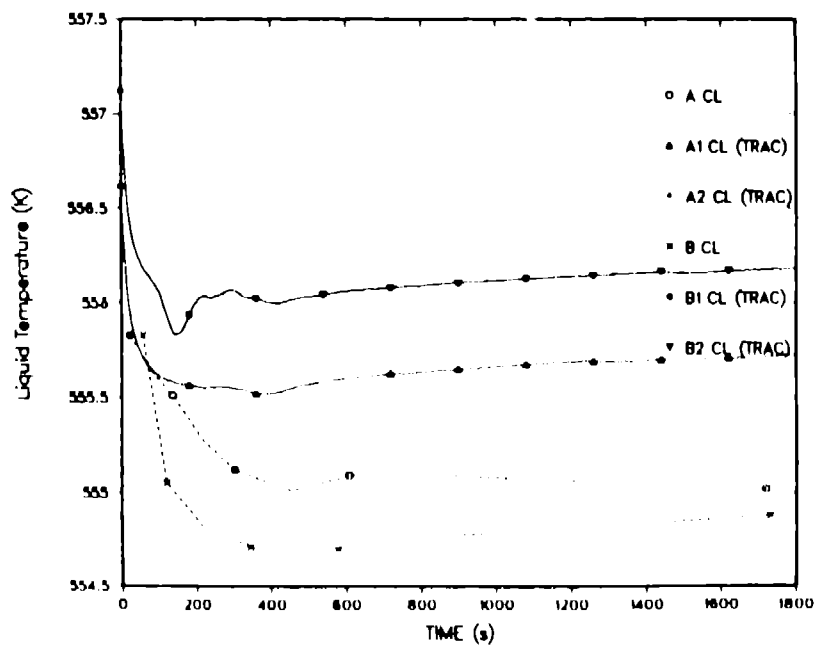


Fig. 15.
Cold leg temperatures for TMI natural circulation test.

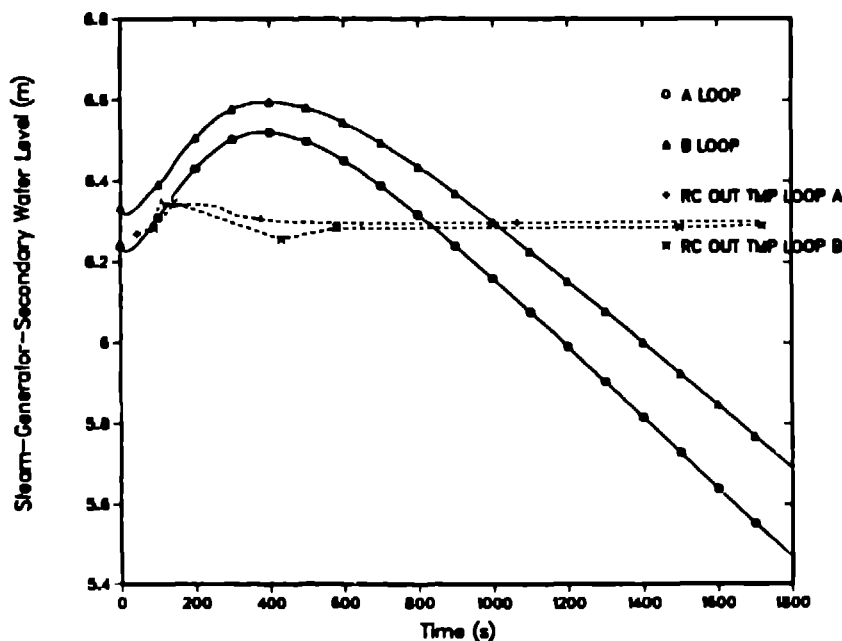


Fig. 16.
OTSG secondary collapsed liquid levels for TMI natural circulation test.

TMI deck are generic curves for lowered loop B&W plants, which do not account for minor differences in pump performance for a specific plant. More accurate modeling of the low-speed pump performance or pump bearing friction would probably improve the calculated natural circulation flow (Fig. 13) and hot-leg temperature (Fig. 14) comparisons after the pump coastdown at approximately 800 s. Differences between the calculation and the test could also be explained by the uncertainty in the core power. Core power data were only available for the first 900 s of the test; if the power assumed in the calculation after this time were too low, then the calculated hot-leg temperatures would also be too low, as shown in Fig. 14.

The uncertainty in the measured OTSG AFW and steam flows does not appear to have caused differences between the calculation and the test. The AFW flows in the test were below the flow instrument range, and the strip chart recordings of the AFW flows show oscillations between 0 and 200 gpm. In addition, there were no steam flow measurements during the test although the TBV stem position was recorded. Even though the maximum indicated value of 200 gpm was used in the calculation, the calculated OTSG secondary levels decreased below the measured levels (Fig. 16) after about 900 s. The OTSG level comparison in Fig. 16 indicates that both the calculated AFW flow and the secondary levels were too low, and therefore the OTSG thermal center elevation was also too low in the calculation. An improved representation of the AFW flow in the calculation would thus increase the calculated thermal center and corresponding natural circulation flow. Since the natural circulation flow was already too high in the calculation (Fig. 13), differences between the calculation and the test cannot be attributed to uncertainty in the measured AFW and steam flows.

The comparison of the benchmark calculation to the natural circulation test results confirms that the TRAC-PF1/MOD2 code and model used for the sensitivity calculations can calculate the OTSG behavior with reasonable accuracy. The overall trends of the transition from forced to natural circulation flow in the test were captured in the calculation, and the differences between measured and calculated parameters were small. Further qualification of the code and model would require additional experimental data over a wider range of operating conditions.

IV. CONCLUSIONS

The matrix of sensitivity calculations and parameter variations was chosen to define the sensitivity of the calculated OTSG and primary system behavior to variations over the range of uncertainty in parameters representing phenomena in the OTSG secondaries. The results of the calculations confirmed the expected sensitivity and quantified the effects of the parameter variations on calculated primary and secondary behavior. The results thus provide information for determining whether additional experimental data are needed in order to improve the accuracy of calculated OTSG behavior. That determination, however, is beyond the scope of this study.

The results of the BCM mapping calculations show that the condensation heat transfer during AFW BCM is nearly proportional to the assumed tube wetting fraction. This sensitivity indicates a need for data to characterize the AFW tube wetting profile. In plant calculations, however, the condensation heat transfer during BCM reduces the vapor pressure inside the tubes, allowing liquid to rise in the tubes and thereby reducing the condensation surface area. This is, therefore, a self-correcting phenomenon. Also, if the OTSG and/or primary system are not rejecting the core heat, then the primary system inventory in a small-break loss-of-coolant accident would continue to deplete and expose more surface area for condensation. The need for wetting profile data is somewhat diminished by this self-limiting/self-correcting characteristic of BCM in plant transients.

Three steam-generator overfill sensitivity calculations were performed which included a base case with no interfacial heat-transfer changes and two sensitivity calculations, one with a multiplier of 0.1 and one with a multiplier of 3 applied to the interfacial heat transfer in the OTSG secondaries. The results of the overfill sensitivity calculations showed that the primary heat removal rate increased with increased interfacial heat transfer, as expected, but the magnitude of the sensitivity was very small.

Interfacial heat transfer in the OTSG secondaries was varied in the MSLB sensitivity calculations. The three MSLB calculations included a base case calculation with no interfacial drag changes and sensitivity calculations with multipliers of 0.001 and 1000 for the drag. The variations in interfacial drag in the MSLB calculations represented not only the uncertainty in the liquid vapor drag coefficient, but also uncertainty in the magnitude of the effects of the entrainment/de entrainment process at the tube support plates and cross flow at the exit in the OTSG secondaries. The results of the MSLB calculations showed a large sensitivity in the OTSG behavior and primary response to variations in interfacial drag. Based on these results and results of the overfill calculations, experimental data to characterize interfacial drag and the entrainment/de entrainment process (for which no models exist) are needed more than data to characterize interfacial heat transfer.

The TRAC-PF1/MOD2 code and model used for the sensitivity calculations were qualified by performing a benchmark calculation for a natural circulation test in the TMI plant. Results of the calculation indicated that the calculated natural circulation flow rate was within the uncertainty of the measured flow rate and, therefore, that the OTSG thermal center elevation was accurately calculated for the conditions in the TMI test. Further qualification of the code and model would require additional experimental data for a wider range of conditions.

The decision of whether additional experimental data are needed to characterize OTSG behavior must ultimately be based on an evaluation of the existing experimental data base and the accuracy of current calculations of OTSG behavior vs the desired accuracy of the calculations. The following observations are provided to assist in defining facility needs, if the decision is made that additional experimental data are needed.

The OTSG behavior is calculated in TRAC-PF1/MOD2 using models and correlations for microscopic physical phenomena. The models are evaluated by the code for cells and junctions representing small regions of the OTSG secondary. The typical OTSG nodalization forces the code to average microscopic processes that occur simultaneously within a cell such as falling film and dispersed droplet heat transfer at tube surfaces, localized effects of the tube support plates in the presence of fully developed flow in the tube bundles, and turning flows that cause some of the droplets to de-entrain on the tube surfaces. On the other hand, some of the processes in the secondary, such as AFW tube wetting, occur over large regions modeled by several cells.

There are three basic methods for improving the accuracy of OTSG calculations. First, additional data could be obtained to better characterize the microscopic physical phenomena or to characterize phenomena for which there are no data, such as de-entrainment of droplets at the tube support plates. With improved characterization of microscopic phenomena, smaller cells could be used for a more accurate representation of the phenomena in code calculations. This approach would use separate effects test facilities to obtain data for microscopic phenomena. The second method would be to develop integrated correlations that include the effects of several phenomena. This method would improve the accuracy of OTSG calculations without requiring the use of smaller cells and would also use separate effects test facilities. The third method is to use a large scale test facility to obtain data to characterize the behavior of a large region of the secondary when a macroscopic process is taking place, develop a correlation from the data, and include the correlation as code option.

If either the first or second methods are chosen, a large scale test facility would still be needed to verify that the correlation improvements based on separate effects facility data actually result in a more accurate calculation of the OTSG performance. The third approach involves a large scale test facility by definition. Therefore, it appears that a large scale test facility would be required regardless of which method is chosen to improve the accuracy of the calculated OTSG behavior.

REFERENCES

1. H. Asaka, "Optimization of TRAC PF1 Condensation Heat Transfer Models for Analysis of Emergency Core Coolant Injection Transients," presented at 2D/3D Coordination Meeting, JAERI, Tokai, Japan, May 9-11, 1988.

2. Safety Code Development Group. "TRAC-PF1/MOD1: An Advanced Best-Estimate Computer Program for Pressurized Water Thermal-Hydraulic Analysis." Los Alamos National Laboratory report LA-10157-MS (NUREG/CR-3858) (July 1986).
3. B. E. Boyack, H. J. Stumpf, and J. F. Lime, "TRAC User's Guide," Los Alamos National Laboratory report LA-10590-M (NUREG/CR-4442) (November 1985).
4. D. R. Liles, J. W. Spore, T. D. Knight, R. A. Nelson, M. W. Cappiello, K. O. Pasamehmetoglu, et al., "TRAC-PF1/MOD1 Correlations and Models," Los Alamos National Laboratory report LA-11208-MS (NUREG/CR-5069) (to be published).
5. J. R. Ireland, et al., "TRAC Analyses of Severe Overcooling Transients for the Oconee-1 PWR", Los Alamos National Laboratory report LA-10055-MS (NUREG/CR-3706) (May 1985).
6. "Benchmarks for AFW (EFW) Models," B&W Document #12-1132555 (April 1982) (Proprietary).
7. T. D. Knight, "Detailed OTSG Calculation," presented at MIST PMG Meeting No. 15. Washington, DC, June 16, 1987.